Efficiently simulating **quarkonium's master equation** beyond the dipole approximation.

Jorge M. Mtz-Vera
jorgemanuel.martinezvera@unito.it
Andrea Beraudo, Paolo Parotto, Miguel Ángel Escobedo, Michael Strickland

UNIVERSITÀ DI TORINO
INFN TORINO
UNIVERSITAT DE BARCELONA
INFN LNS Istituto Nazionale di Fisica Nucleare Laboratori Nazionali del Sud

Quarkonia as an OQS

Can we describe how quarkonia propagates through a medium *from first principles*?

Quarkonia as an OQS

Can we describe how quarkonia propagates through a medium *from first principles*?

Open Quantum Systems can help us outline a method to do so.

Quarkonia as an OQS

Can we describe how quarkonia propagates through a medium *from first principles*?

Open Quantum Systems can help us outline a method to do so.

Can we do it *efficiently*?

Quarkonia as an OQS

Can we describe how quarkonia propagates through a medium *from first principles*?

Open Quantum Systems can help us outline a method to do so.

Can we do it *efficiently*?

We can try! Taking advantage of the symmetries of the problem.

Quarkonia

They are **bound states of a heavy quark-antiquark pair ($Q\bar{Q}$) of the same kind** (Olsen et al., 2017) which are stable with respect to strong decay into open charm/bottom (Sarkar et al., 2010).

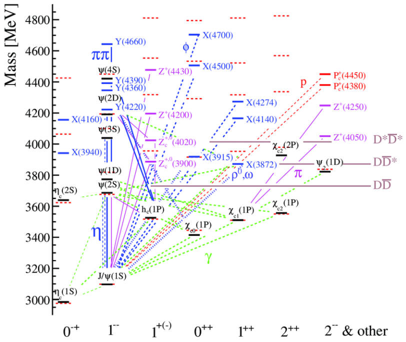

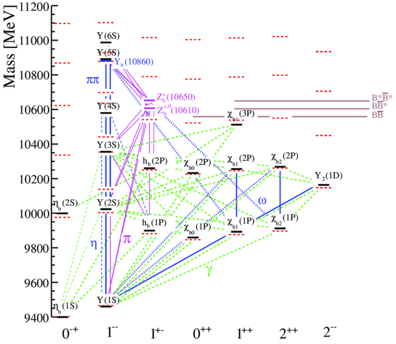

Observations

Experimental evidence (Chatrchyan et al., 2012) of nuclear effects in the creation and propagation of quarkonia.

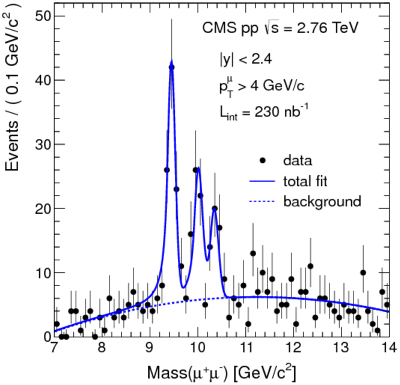

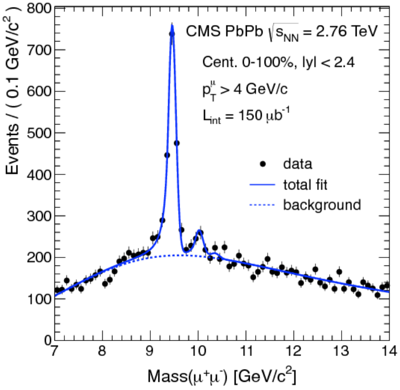

Why quarkonia as a probe

1. Well-known probe. Experimentally, clean signal through dilepton decays.
2. Hard scale: quarkonia mass $m_{Q\bar{Q}}, m_Q \gg \Lambda_{QCD}$. *Easy* to be described by EFT.
3. Small radius: harder to dissociate from color screening than light quark matter.

(Roland Katz, 2015)

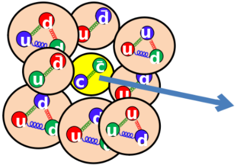

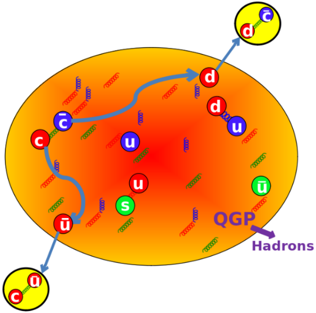

Open Quantum Systems 101

We divide the full quantum system (T) into well-differentiated parts: the subsystem (S) and the environment (E) (Breuer and Petruccione, 2002).

The full quantum dynamics of the subsystem is kept whereas the environment is traced out.

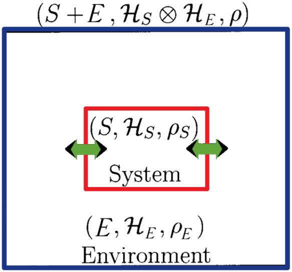

Main character (**density matrix**, ρ) and **observables** $\langle \mathcal{O} \rangle$:

$$\rho = \sum_i p_i \left|\psi_i\right\rangle \left\langle\psi_i\right| \longrightarrow \langle \mathcal{O} \rangle = Tr\{\rho \mathcal{O}\}.$$

Open Quantum Systems 101

We divide the full quantum system (T) into well-differentiated parts: the subsystem (S) and the environment (E) (Breuer and Petruccione, 2002).

The full quantum dynamics of the subsystem is kept whereas the environment is traced out.

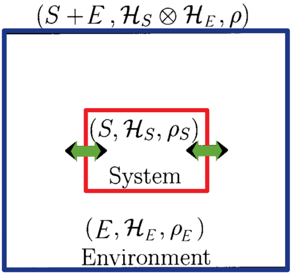

Main character (**density matrix**, ρ) and **observables** $\langle\mathcal{O}\rangle$:

$$\rho=\sum_i p_i\left|\psi_i\right\rangle\left\langle\psi_i\right|\longrightarrow\langle\mathcal{O}\rangle=Tr\{\rho\mathcal{O}\}.$$

Reduced density matrix: $\mathrm{tr}_E\{\rho_T\}=\rho_S\longrightarrow\langle\mathcal{O}\rangle=Tr_S\{\rho_S\mathcal{O}\}.$

Open Quantum Systems 101

We divide the full quantum system (T) into well-differentiated parts: the subsystem (S) and the environment (E) (Breuer and Petruccione, 2002).

The full quantum dynamics of the subsystem is kept whereas the environment is traced out.

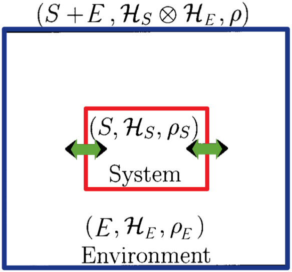

Main character (**density matrix**, ρ) and **observables** $\langle\mathcal{O}\rangle$:

$$\rho = \sum_i p_i \left|\psi_i\right\rangle \left\langle\psi_i\right| \longrightarrow \langle\mathcal{O}\rangle = Tr\{\rho\mathcal{O}\}.$$

Reduced density matrix: $\mathrm{tr}_E\{\rho_T\} = \rho_S \longrightarrow \langle\mathcal{O}\rangle = Tr_S\{\rho_S\mathcal{O}\}$.

Hamiltonian: $H_T = H_S \otimes \mathbb{I}_E + \mathbb{I}_S \otimes H_E + H_I$, where $H_I = V_S \otimes V_E$.

Open Quantum Systems for Quarkonia

The explicit form of the full hamiltonian (using LO NRQCD in the Coulomb gauge) would be:

$$\begin{aligned} H_T = T_{kin}^{Q\bar{Q}} - C_F \alpha_s m_D + V_x(|\mathbf{x}_{\bar{Q}} - \mathbf{x}_Q|) \otimes \mathbb{I}_E + \mathbb{I}_S \otimes H_{q+A} \\ + \int d^3x [\delta(\mathbf{x} - \mathbf{x}_Q) t_Q^a - \delta(\mathbf{x} - \mathbf{x}_{\bar{Q}}) t_{\bar{Q}}^{a*}] \otimes g A_0^a(\mathbf{x}) \end{aligned} \quad (1)$$

Open Quantum Systems for Quarkonia

The explicit form of the full hamiltonian (using LO NRQCD in the Coulomb gauge) would be:

$$\begin{aligned} H_T = T_{kin}^{Q\bar{Q}} - C_F \alpha_s m_D + V_x(|\mathbf{x}_{\bar{Q}} - \mathbf{x}_Q|) \otimes \mathbb{I}_E + \mathbb{I}_S \otimes H_{q+A} \\ + \int d^3x [\delta(\mathbf{x} - \mathbf{x}_Q) t_Q^a - \delta(\mathbf{x} - \mathbf{x}_{\bar{Q}}) t_{\bar{Q}}^{a*}] \otimes g A_0^a(\mathbf{x}) \end{aligned} \tag{1}$$

We know that:

$$Tr_E \Big[T[A_0^a(t_1, \mathbf{x}_1) A_0^b(t_2, \mathbf{x}_2)] \rho_E \Big] = -i \delta^{ab} \Delta(t_1 - t_2, \mathbf{x}_1 - \mathbf{x}_2)$$

Open Quantum Systems for Quarkonia

The explicit form of the full hamiltonian (using LO NRQCD in the Coulomb gauge) would be:

$$H_T = T_{kin}^{Q\bar{Q}} - C_F \alpha_s m_D + V_x(|\mathbf{x}_{\bar{Q}} - \mathbf{x}_Q|) \otimes \mathbb{I}_E + \mathbb{I}_S \otimes H_{q+A} \\ + \int d^3x [\delta(\mathbf{x} - \mathbf{x}_Q) t_Q^a - \delta(\mathbf{x} - \mathbf{x}_{\bar{Q}}) t_{\bar{Q}}^{a*}] \otimes g A_0^a(\mathbf{x}) \quad (1)$$

We know that:

$$Tr_E \Big[T[A_0^a(t_1, \mathbf{x}_1) A_0^b(t_2, \mathbf{x}_2)] \rho_E \Big] = -i \delta^{ab} \Delta(t_1 - t_2, \mathbf{x}_1 - \mathbf{x}_2)$$

We can profit from the fact that propagators of the A_0 component can be linked with real and imaginary potentials like (Blaizot and Escobedo, 2017):

$$V(\mathbf{r}) = -\Delta^R(\omega = 0, \mathbf{r}), \qquad W(\mathbf{r}) = -\Delta^<(\omega = 0, \mathbf{r})$$

Timescales

These approximations also refer to the characteristic timescales τ_i of the different parts of the system, namely:

$$\tau_S = 1/\Delta E, \quad \tau_E \sim 1/T, \quad \tau_R \sim M/T^2.$$

Here ΔE is the energy gap between the energy levels of the bound state, T is the temperature and M is the particle mass.

Timescales

These approximations also refer to the characteristic timescales τ_i of the different parts of the system, namely:

$$\tau_S = 1/\Delta E, \quad \tau_E \sim 1/T, \quad \tau_R \sim M/T^2.$$

Here ΔE is the energy gap between the energy levels of the bound state, T is the temperature and M is the particle mass.

We look for the regime where:

$$\tau_E \ll \tau_R \longrightarrow \text{Born and Markov approximations,}$$

$$\tau_E \ll \tau_S \longrightarrow \text{Born-Oppenheimer approximation.}$$

These considerations will help out with the algebraic manipulations to reach the desired and consistent OQS shape of the equation of evolution.

Evolution equation.

Starting point: Liouville-von Neumann equation: $\frac{d\rho_T}{dt} = -i\,[H_T, \rho_T]$

- Trace over environment degrees of freedom: $\mathrm{tr}_E \left\{ \frac{d\rho_T}{dt} \right\}$.
- Born, Markov and Born-Oppenheimer approximations $\longrightarrow$ Brownian motion regime.

  Lindblad equation:

$$\frac{d\rho_S}{dt} = -i\,[H_S, \rho_T] + \sum_k \left(C_k \rho_S C_k^\dagger - \frac{1}{2}\{C_k^\dagger C_k, \rho_S\} \right)$$

Evolution equation.

Starting point: Liouville-von Neumann equation: $\frac{d\rho_T}{dt} = -i\left[H_T, \rho_T\right]$

- Trace over environment degrees of freedom: $\mathrm{tr}_E\left\{\frac{d\rho_T}{dt}\right\}$.
- Born, Markov and Born-Oppenheimer approximations $\longrightarrow$ Brownian motion regime.

  Lindblad equation:

$$\frac{d\rho_S}{dt} = -i\left[H_S, \rho_T\right] + \sum_k \left(C_k \rho_S C_k^\dagger - \frac{1}{2}\{C_k^\dagger C_k, \rho_S\}\right)$$

The task left is solving it! $\Longrightarrow$ QTRAJ1.0

1. High computational cost.
2. Current implementation works in the dipole approximation, where $rT \ll 1$.

Quantum trajectories: an algorithm to solve Lindblad's.

We redefine the subsystem hamiltonian by adding an immaginary component coming from the anti-commutators (Akamatsu, 2022; Blaizot and Escobedo, 2018; Yao and Mehen, 2019).
It becomes a **non-hermitian hamiltonian.**

$$H_{eff} = H_S - \frac{i}{2}\sum_x \int_{\boldsymbol{q}} \underbrace{C^\dagger_{\boldsymbol{q},x} C_{\boldsymbol{q},x}}_{\Gamma_{\boldsymbol{q},x}} = H_S - \frac{i}{2}\Gamma.$$

$$\boxed{\frac{d\rho_S}{dt} = -i[H_{eff}(t), \rho_S]} + \sum_x \int_{\boldsymbol{q}} C_{\boldsymbol{q},x}\rho_S C^\dagger_{\boldsymbol{q},x},$$

The state is evolved in Schrödinger-like way (norm decreases).
When the norm goes below a certain value, a projection (jump) is performed according to certain selection rules.
QTRAJ1.0 (+ 0.1) is a C-based code using this scheme on the **wavefunction** in order to retrieve the final population of quarkonia.

Upgrade of the jump operators with respect to QTRAJ 1.0

We may identify some of the new families of operators with the previous finite number of operators.

$$C_i^0 = \sqrt{\frac{\kappa}{N_c^2-1}}\hat{r}_i \begin{pmatrix} 0 & 1 \\ \sqrt{N_c^2-1} & 0 \end{pmatrix} \longrightarrow C_{\boldsymbol{q}}^0 = \begin{pmatrix} 0 & \frac{1}{\sqrt{2N_c}} L_{\boldsymbol{q}} \\ \sqrt{C_F} L_{\boldsymbol{q}} & 0 \end{pmatrix},$$

$$C_i^1 = \sqrt{\frac{(N_c^2-4)\kappa}{2(N_c^2-1)}}\hat{r}_i \begin{pmatrix} 0 & 0 \\ 0 & 1 \end{pmatrix} \longrightarrow C_{\boldsymbol{q}}^1 = \begin{pmatrix} 0 & 0 \\ 0 & \sqrt{\frac{N_c^2-4}{4N_c}} L_{\boldsymbol{q}} \end{pmatrix},$$

$$\text{NEW!} \longrightarrow C_{\boldsymbol{q}}^2 = \begin{pmatrix} 0 & 0 \\ 0 & \frac{\sqrt{N_c}}{2} \bar{L}_{\boldsymbol{q}} \end{pmatrix},$$

where

$$L_{\boldsymbol{q}} = L_{\boldsymbol{q}}^\dagger = 2g\sqrt{\Delta^<(\boldsymbol{q},0)} \sin\frac{\boldsymbol{q}\cdot\hat{\boldsymbol{r}}}{2},$$

$$\bar{L}_{\boldsymbol{q}} = \bar{L}_{\boldsymbol{q}}^\dagger = 2g\sqrt{\Delta^<(\boldsymbol{q},0)} \cos\frac{\boldsymbol{q}\cdot\hat{\boldsymbol{r}}}{2}.$$

Splitting in the colour basis.

- Splitting in a color basis (singlet-octet).

$$\rho_S(t) = \rho_s(t) |s\rangle \langle s| + \bar{\rho}_o(t) \sum_C |o_C\rangle \langle o_C| \Longrightarrow$$

$$\underbrace{(N_c^2 - 1)\bar{\rho}_o(t)}_{\rho_o} \underbrace{\sum_C \frac{1}{N_c^2 - 1} |o_C\rangle \langle o_C|}_{\text{average}} = \rho_o(t) |o\rangle \langle o| \,.$$

Splitting in the colour basis.

- Splitting in a color basis (singlet-octet).

$$\rho_S(t) = \rho_s(t)\,|s\rangle\langle s| + \bar{\rho}_o(t)\sum_C |o_C\rangle\langle o_C| \Longrightarrow$$

$$\underbrace{(N_c^2-1)\bar{\rho}_o(t)}_{\rho_o}\underbrace{\sum_C \frac{1}{N_c^2-1}|o_C\rangle\langle o_C|}_{\text{average}} = \rho_o(t)\,|o\rangle\langle o|\,.$$

We rewrite the previous equation as the system:

$$\frac{d\rho_s}{dt} = -iH^s_{\text{eff}}\rho_s + i\rho_s H^{s\dagger}_{\text{eff}} + C_F\int_{\boldsymbol{q}} L_{\boldsymbol{q}}\rho_o L_{\boldsymbol{q}},$$

$$\frac{d\rho_o}{dt} = -iH^o_{\text{eff}}\bar{\rho}_o + i\rho_o H^{o\dagger}_{\text{eff}} + \frac{1}{2N_c}\int_{\boldsymbol{q}} L_{\boldsymbol{q}}\rho_s L_{\boldsymbol{q}} + \frac{N_c^2-4}{4N_c}\int_{\boldsymbol{q}} L_{\boldsymbol{q}}\rho_o L_{\boldsymbol{q}} + \frac{N_c}{4}\int_{\boldsymbol{q}} \bar{L}_{\boldsymbol{q}}\rho_o \bar{L}_{\boldsymbol{q}}.$$

When is a jump triggered?

Due to the non-hermitian nature of the hamiltonian $\implies$ the norm decreases.
A zeroth random number is drawn r_0. When the condition:

$$r_0 > |\langle \psi(t_i) | \psi(t_i) \rangle|,$$

the jump is triggered and the selection rules come into play.

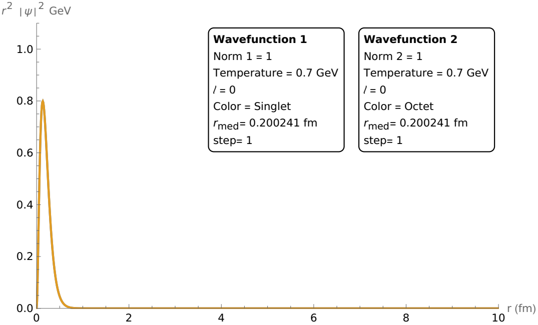

When is a jump triggered?

Due to the non-hermitian nature of the hamiltonian $\Longrightarrow$ the norm decreases.
A zeroth random number is drawn r_0. When the condition:

$$r_0 > |\langle\psi(t_i)|\psi(t_i)\rangle|,$$

the jump is triggered and the selection rules come into play.

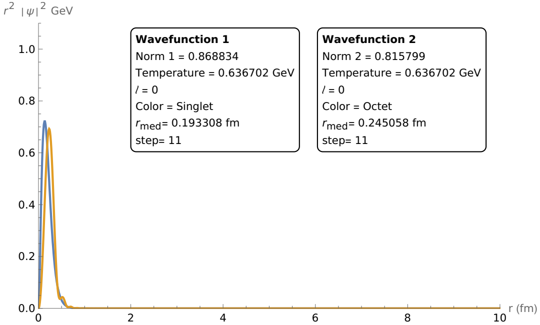

When is a jump triggered?

Due to the non-hermitian nature of the hamiltonian $\Longrightarrow$ the norm decreases.
A zeroth random number is drawn r_0. When the condition:

$$r_0 > |\langle\psi(t_i)|\psi(t_i)\rangle|,$$

the jump is triggered and the selection rules come into play.

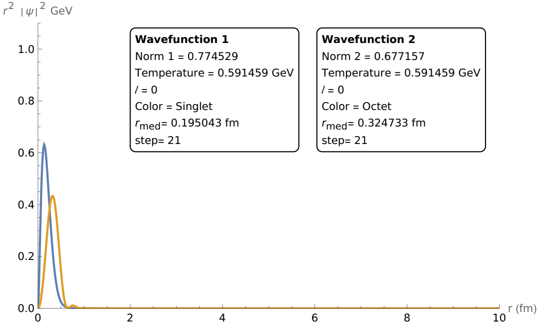

When is a jump triggered?

Due to the non-hermitian nature of the hamiltonian $\Longrightarrow$ the norm decreases.
A zeroth random number is drawn r_0. When the condition:

$$r_0 > |\langle\psi(t_i)|\psi(t_i)\rangle|,$$

the jump is triggered and the selection rules come into play.

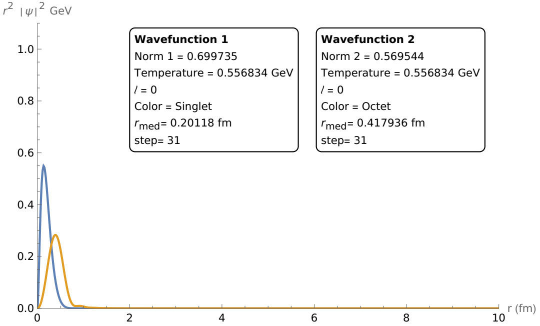

When is a jump triggered?

Due to the non-hermitian nature of the hamiltonian $\Longrightarrow$ the norm decreases.
A zeroth random number is drawn r_0. When the condition:

$$r_0 > |\langle \psi(t_i) | \psi(t_i) \rangle|,$$

the jump is triggered and the selection rules come into play.

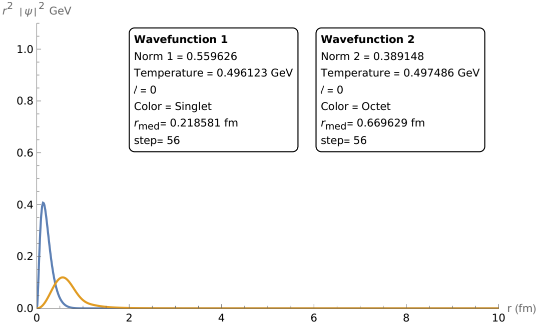

When is a jump triggered?

Due to the non-hermitian nature of the hamiltonian $\implies$ the norm decreases.
A zeroth random number is drawn r_0. When the condition:

$$r_0 > |\langle\psi(t_i)|\psi(t_i)\rangle|,$$

the jump is triggered and the selection rules come into play.

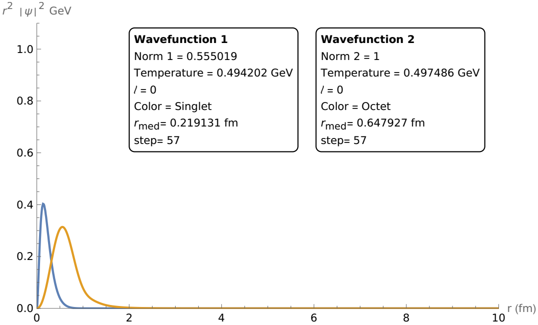

Selection rules.

QTRAJ 1.0 $\rightarrow$ 2 Selection rules independent of the wavefunction.

$$p(s \rightarrow o) = 1; \quad p(o \rightarrow s) = 2/7.$$

QTRAJ 1.1 $\rightarrow$ 4 selection rules depending on the shape of the wavefunction.

1. Color state: singlet/octet $\rightarrow r_1$.
2. Maximum angular momentum exchanged, $t \rightarrow r_2$.
3. Angular momentum of the final state $\rightarrow r_3$.
4. Linear impulse exchanged by the propagator $\rightarrow r_4$.

The probability of jumping to a specific final state depends on $p(i \longrightarrow f) = p(r_1, r_2, r_3, r_4)$.

1 Color state: singlet/octet, Γ^s; $\Gamma^o = \Gamma^{o_1} + \Gamma^{o_2} + \Gamma^{o_3}$.

$$p(s \to o) = 1; \quad p_i(o \to x) = \frac{\Gamma^{o_i}}{\Gamma^o} \quad \text{where} \quad x = \{s, o\}.$$

Draw a first random number, r_1. Choose i to be the lowest value for which the following is satisfied:

$$0 \leq p_1 < p_1 + p_2 \leq p_1 + p_2 + p_3 = 1.$$

We will call the chosen decay width, generically, Γ^x.

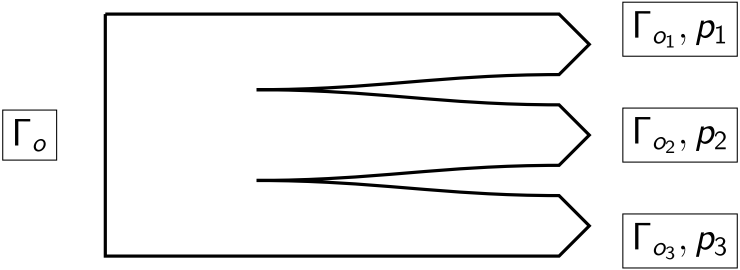

2 Maximum angular momentum exchanged, t, of $L_{\boldsymbol{q}}$ and $\bar{L}_{\boldsymbol{q}}$, *v.g.*:

$$L_{\boldsymbol{q}} = L_{\boldsymbol{q}}^{\dagger} = 2g\sqrt{\Delta^{<}(\boldsymbol{q},0)}\sin\frac{\boldsymbol{q}\cdot\hat{\boldsymbol{r}}}{2} \Longrightarrow \Gamma = \int_{\boldsymbol{q}} L_{\boldsymbol{q}} L_{\boldsymbol{q}}^{\dagger}.$$

$$\Gamma = \sum_t \Gamma_t = A\int_q q^2\Delta^{<}(q)(4t+3)\left[j_{2t+1}(q\hat{r}/2)\right]^2 \Longrightarrow r_2 < \frac{1}{\Gamma^x}\sum_{i=0}^{t}\Gamma_i^x.$$

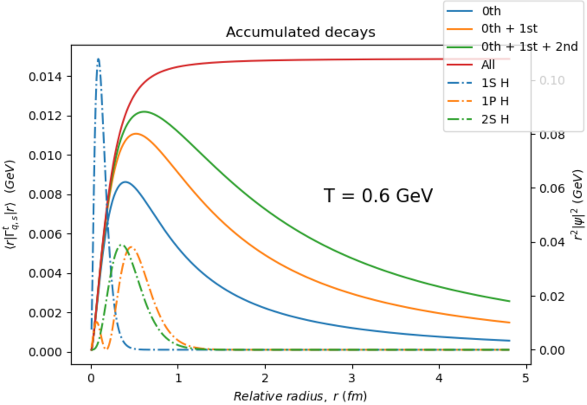

3 Angular momentum of the final state.

$$p(\ell_i \to \ell_f) = \frac{\sum_{m_i,m,m_f} \frac{1}{(2\ell_f+1)} |\langle \ell_i, 0; 2t+1, 0|\ell_f, 0\rangle|^2 |\langle \ell_i, m_i; 2t+1, m|\ell_f, m_f\rangle|^2}{\sum_{m_i',m',\ell_f',m_f'} \frac{1}{(2\ell_f'+1)} |\langle \ell_i, 0; 2t+1, 0|\ell_f', 0\rangle|^2 |\langle \ell_i, m_i'; 2t+1, m'|\ell_f', m_f'\rangle|^2}$$

$$r_3 < \sum_{\ell=0}^{\ell_f} p(d \to \ell).$$

4 Linear impulse exchanged by the propagator (modulus).

$$PDF \to \frac{d\Gamma}{d\boldsymbol{q}} = q^2 \Delta^<(q)(4t+3)\left[j_{2t+1}(q\hat{r}/2)\right]^2,$$

$$q_{chosen} = CDF^{-1}(r_4).$$

The order of these steps may in principle be exchanged (currently under testing).

Final state

$$|\psi_{new}\rangle = \frac{C^n_{\boldsymbol{q}} |\psi_{old}\rangle}{\sqrt{\langle\psi_{old}| \Gamma^n_{\boldsymbol{q}} |\psi_{old}\rangle}}$$

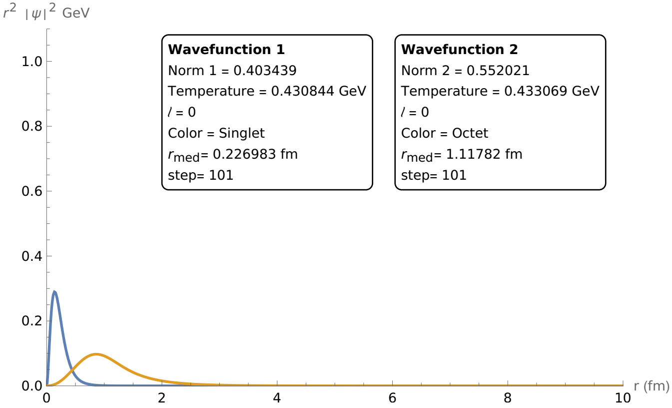

Final state

$$|\psi_{new}\rangle = \frac{C^n_{\boldsymbol{q}} |\psi_{old}\rangle}{\sqrt{\langle\psi_{old}| \Gamma^n_{\boldsymbol{q}} |\psi_{old}\rangle}}$$

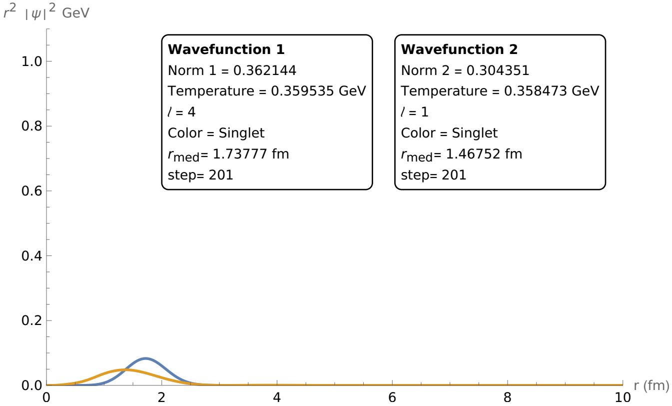

Final state

$$|\psi_{new}\rangle = \frac{C^n_{\boldsymbol{q}} |\psi_{old}\rangle}{\sqrt{\langle\psi_{old}| \Gamma^n_{\boldsymbol{q}} |\psi_{old}\rangle}}$$

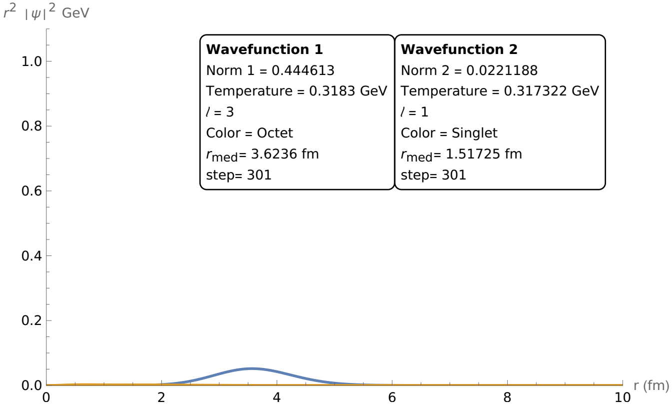

Final state

$$|\psi_{new}\rangle = \frac{C_{\boldsymbol{q}}^{n} |\psi_{old}\rangle}{\sqrt{\langle\psi_{old}| \Gamma_{\boldsymbol{q}}^{n} |\psi_{old}\rangle}}$$

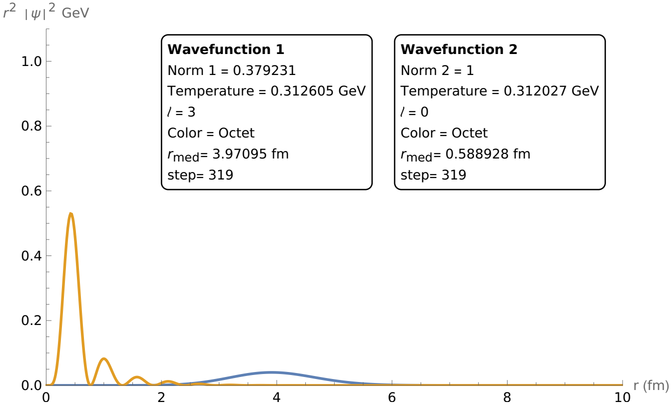

Final state

$$|\psi_{new}\rangle = \frac{C_{\boldsymbol{q}}^{n} |\psi_{old}\rangle}{\sqrt{\langle\psi_{old}| \Gamma_{\boldsymbol{q}}^{n} |\psi_{old}\rangle}}$$

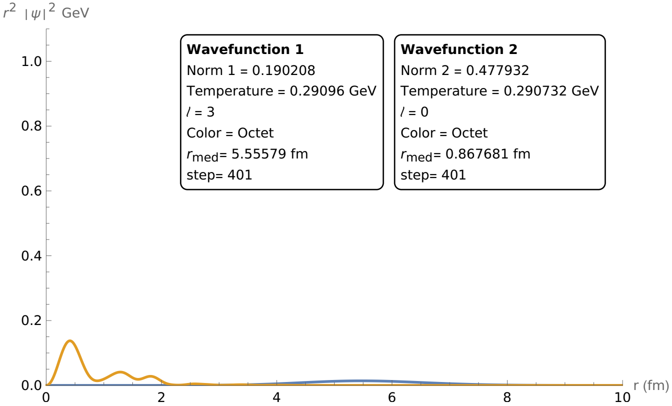

Conclusions.

1. The inclusion of less restrictive potentials allows the expansion the regime of validity of the simulations to $rT \sim 1$.
2. A whole new family of operators is included. These, in contrast to previous implementations, allow transitions preserving the parity of the initial state.
3. The repulsive nature of the octet potential, the radius of the couple tends to be increased, favouring the appearance of transitions of $\Delta\ell > 1$, which before were forbidden.

References I

Stephen Olsen, Tomasz Skwarnicki, and Daria Zieminska.
Non-standard heavy mesons and baryons, an experimental review.
08 2017.

Sourav Sarkar, Helmut Satz, and Bikash Sinha, editors.
The physics of the quark-gluon plasma, volume 785.
2010.

Serguei Chatrchyan et al.
Observation of Sequential Upsilon Suppression in PbPb Collisions.
Phys. Rev. Lett., 109:222301, 2012.
[Erratum: Phys.Rev.Lett. 120, 199903 (2018)].

Sarah Porteboeuf.
Short description of retequarkonii activities.
https://twiki.cern.ch/twiki/bin/view/ReteQuarkonii/ReteQuarkonii.
Accessed: 2023-09-26.

Roland Katz and Pol Bernard Gossiaux.
The Schrödinger–Langevin equation with and without thermal fluctuations.
Annals Phys., 368:267–295, 2016.

H. P. Breuer and F. Petruccione.
The theory of open quantum systems.
2002.

Jean-Paul Blaizot and Miguel Angel Escobedo.
Quantum and classical dynamics of heavy quarks in a quark-gluon plasma.
JHEP, 06:034, 2018.

References II

Yukinao Akamatsu.
Quarkonium in quark–gluon plasma: Open quantum system approaches re-examined.
Prog. Part. Nucl. Phys., 123:103932, 2022.

Jean-Paul Blaizot and Miguel Angel Escobedo.
Approach to equilibrium of a quarkonium in a quark-gluon plasma.
Phys. Rev. D, 98(7):074007, 2018.

Xiaojun Yao and Thomas Mehen.
Quarkonium in-medium transport equation derived from first principles.
Phys. Rev. D, 99(9):096028, 2019.

José C. Jiménez.
Interacting quark matter effects on the structure of compact stars.
PhD thesis, Rio de Janeiro Federal U., 2020.

Nora Brambilla, Miguel A. Escobedo, Joan Soto, and Antonio Vairo.
Heavy quarkonium suppression in a fireball.
Phys. Rev. D, 97(7):074009, 2018.

Approximations: Born approximation

It is a weak coupling between the subsystem and the environment, $H_I \ll 1$.

$$\rho_T(t) = \rho_S(t) \otimes \rho_E(t) + \rho_{corr}(t) \approx \rho_S(t) \otimes \rho_E(t),$$

where ρ_{corr} is the correlation component between the environment and the subsystem.

$$\frac{d\rho_{T,I}(t)}{dt} \approx -\int_0^t d\tau [H_I(t), [H_I(\tau), \rho_{S,I}(\tau) \otimes \rho_{E,I}(0)]]$$

Approximations: Markov approximation

Taking into account only the current step in order to obtain the next one $\rho_{S,I}(\tau) \longrightarrow \rho_{S,I}(t)$. We will perform the change of variable $\tau \longrightarrow \tau' = t - \tau$ so:

- $\tau = 0 \longrightarrow \tau' = t - \tau = t$
- $\tau = t \longrightarrow \tau' = t - \tau = 0$
- Since the correlation time of the environment is much less than the average relaxation time of the system we can take $t \longrightarrow \infty$.

If we also trace over the environment, we get:

$$\frac{d\rho_{S,I}(t)}{dt} \approx -\int_0^\infty d\tau \; tr_E\{[H_I(t), [H_I(t-\tau), \rho_{S,I}(t) \otimes \rho_{E,I}(0)]]\}.$$

Redfield equation.

Approximations: Born-Oppenheimer approximation

The environmental degrees of freedom move much faster than the quarkonium so effectively they instantly change to any changes that the quarkonium may induce.

$$V_S(t-s) \approx V_S(t) - s\frac{dV_S(t)}{dt} + \cdots = V_S(t) - is[H_S, V_S(t)] + \ldots$$

Gradient expansion for Brownian motion.

1. Projecting $\rho_S(t)$ into spherical harmonics.
2. Also, split into the singlet-octet colour basis.

$$\rho_S(t) = diag(\rho_S^{sing,s}, \rho_S^{oct,s}, \rho_S^{sing,p}, \rho_S^{oct,p})$$

Great computational advantage: 3D $\longrightarrow$ 1D $\cdot Y_m^{\ell}(\theta, \phi)$.

Quark-gluon plasma

It is a deconfined phase on the QCD phase diagram [11].

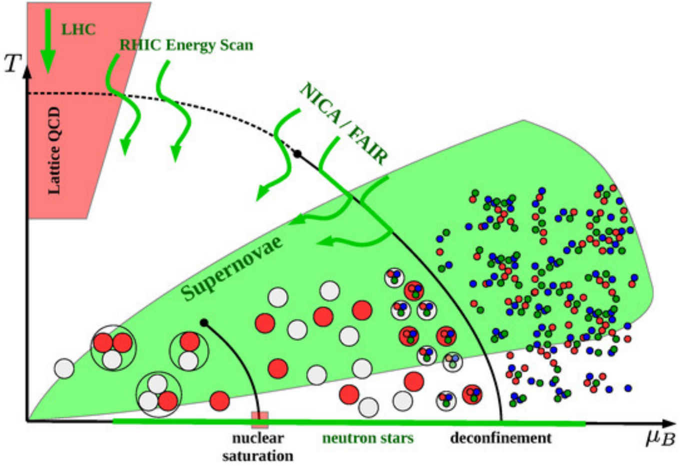

Comparisson with other theorical developments.

For a weakly-coupled plasma (Brambilla et al., 2017) :

$$\left.\begin{aligned} C_i^0 &= \sqrt{\frac{2\left(\mu_E\right)T}{3N_c}}\left[\frac{2ip_i}{M}+\frac{N_c\left(1/a_o\right)r_i}{2r}\right]\begin{pmatrix}0 & 1\\ 0 & 0\end{pmatrix} \\ C_i^1 &= \sqrt{\frac{4C_F\left(\mu_E\right)T}{3}}\left[-\frac{2ip_i}{M}+\frac{N_c\left(1/a_o\right)r_i}{2r}\right]\begin{pmatrix}0 & 0\\ 1 & 0\end{pmatrix}\end{aligned}\right\} C_{\boldsymbol{q}}^0 = \begin{pmatrix}0 & \frac{1}{\sqrt{2N_c}}L_{\boldsymbol{q}} \\ \sqrt{C_F}L_{\boldsymbol{q}} & 0\end{pmatrix}$$

$$C_i^2 = \frac{2}{M}\sqrt{\frac{(N_c^2-4)(\mu_E)T}{3N_c}}p_i\begin{pmatrix}0 & 0\\ 0 & 1\end{pmatrix} \longrightarrow C_{\boldsymbol{q}}^1 = \begin{pmatrix}0 & 0\\ 0 & \sqrt{\frac{N_c^2-4}{4N_c}}L_{\boldsymbol{q}}\end{pmatrix},$$

$$\text{NEW!} \longrightarrow C_{\boldsymbol{q}}^2 = \begin{pmatrix}0 & 0\\ 0 & \frac{\sqrt{N_c}}{2}\bar{L}_{\boldsymbol{q}}\end{pmatrix},$$